SUPPORTING INFORMATION

$SLi_4X_3^-$ (X = Cl, Br, I)：Fan-shaped Superhalogen Anions Featuring Planar Tetracoordinate Sulfur

Ting Zhang,[1] Ya-Xuan Cheng,[2] and Jin-Chang Guo*[2]

[1]Department of Chemistry, Xinzhou Normal University, Xinzhou 034000, China

[2]Institute of Molecular Science, Shanxi University, Taiyuan 030006, China

E-mail: guojc@sxu.edu.cn

Supporting Information

Table S1. The lowest vibrational frequency (ν_{min}, cm^{-1}) at four classical theoretical levels for the global minimum **1**–**3** structures of $SLi_4X_3^-$ (X = Cl, Br, I) clusters.

Table S2. Energy components of IQA for the C_{2v} S©$Li_4X_3^-$ (X = Cl, Br, I) clusters at the PBE0/TZ2P level; V^{IQA}, V_C, and V_{XC} are the interatomic IQA interaction energy and the coulombic and exchange-correlation energy components, respectively, in kcal/mol.

Table S3. AIM parameters (atomic units) for the bond critical points (BCPs) corresponding to the bonds in C_{2v} $SLi_4Cl_3^-$ (**1**) cluster.

Table S4. AIM parameters (atomic units) for the bond critical points (BCPs) corresponding to the bonds in C_{2v} $SLi_4Br_3^-$ (**2**) cluster.

Table S5. AIM parameters (atomic units) for the bond critical points (BCPs) corresponding to the bonds in C_{2v} $SLi_4I_3^-$ (**3**) cluster.

Figure S1. The AdNDP bonding pattern of $SLi_4Br_3^-$ (**2**) with occupation numbers (ONs, in |e|). (a) Nine lone pairs (LPs) of three Br atoms; (b) Three LPs of the S center; (c) Three 3c-2e Li–Br–Li σ bonds; (d) One 5c-2e σ bond.

Figure S2. The AdNDP bonding pattern of $SLi_4I_3^-$ (**3**) with occupation numbers (ONs, in |e|). (a) Nine lone pairs (LPs) of three I atoms; (b) Three LPs of the S center; (c) Three

3c-2e Li–I–Li σ bonds; (d) One 5c-2e σ bond.

Figure S3. 2D plots of ELF and the contour line maps of Laplacian of electron density, bond paths and critical points of ptS **2** and **3**. The blue and red solid lines represent the positive and negative regions, respectively. The brown sticks between the atoms represent bond paths. The brown and yellow dots are bond and ring critical points, respectively.

Figure S4. Color-filled maps of $NICS(0)_{ZZ}$ and $NICS(1)_{ZZ}$ of the ptS **2, 3** clusters. 0 and 1 (in Å) represent the height above the molecular plane. Negative values indicate aromaticity.

Cartesian coordinates of the top five low-lying isomers of $SLi_4X_3^-$ (X = Cl, Br, I) at the PBE0-D3(BJ)/def2-TZVPP level.

Table S1. The lowest vibrational frequency (ν_{min}, cm^{-1}) at four classical theoretical levels for the global-minimum **1**–**3** structures of $SLi_4X_3^-$ (X = Cl, Br, I) clusters.

	Theoretical level	ν_{min} (cm^{-1})		
		1	**2**	**3**
1	PBE0-D3(BJ)/def2-TZVPP	10.6	9.3	5.6
2	B2PLYP-D3(BJ)/def2-TZVPP	12.1	7.5	4.6
3	MP2/def2-TZVPP	19.1	15.7	14.4
4	CCSD/def2-TZVPP	19.3	15.7	14.2

Table S2. Energy components of IQA for the C_{2v} $SLi_4X_3^-$ (X = Cl, Br, I) clusters at the PBE0/TZ2P level; V^{IQA}, V_C, and V_{XC} are the interatomic IQA interaction energy and the coulombic and exchange-correlation energy components, respectively, in kcal/mol.

	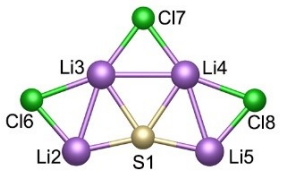 **1** $SLi_4Cl_3^-$ (C_{2v}, $^1A_1$)	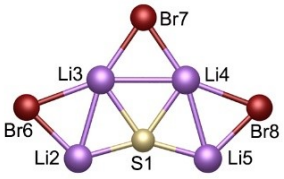 **2** $SLi_4Br_3^-$ (C_{2v}, $^1A_1$)	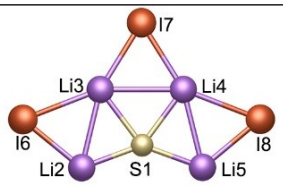 **3** $SLi_4I_3^-$ (C_{2v}, $^1A_1$)
V^{IQA}(S1–Li2)	–237.6	–237.9	–237.2
V_C(S1–Li2)	–218.2 (91.8%)	–218.7 (91.9%)	–218.1 (91.9%)
V_{XC}(S1–Li2)	–19.4 (8.2%)	–19.2 (8.1%)	–19.1 (8.1%)
V^{IQA}(S1–Li3)	–218.1	–222.8	–222.5
V_C(S1–Li3)	–207.4 (95.1%)	–211.0 (94.7%)	–210.0 (94.4%)
V_{XC}(S1–Li3)	–10.7 (4.9%)	–11.8 (5.3%)	–12.5 (5.6%)
V^{IQA}(Li2–Li3)	100.9	98.3	95.2
V_C(Li2–Li3)	101.0 (99.9%)	98.4 (99.9%)	95.3 (99.9%)
V_{XC}(Li2–Li3)	–0.1 (0.1%)	–0.1 (0.1%)	–0.1 (0.1%)
V^{IQA}(Li3–Li4)	96.2	94.6	90.8
V_C(Li3–Li4)	96.3 (99.9%)	94.7 (99.9%)	90.9 (99.9%)
V_{XC}(Li3–Li4)	–0.1 (0.1%)	–0.1 (0.1%)	–0.1 (0.1%)
V^{IQA}(Li2–X6)	–145.0	–137.8	–128.4
V_C(Li2–X6)	–129.6 (89.4%)	–123.1 (89.3%)	–115.3 (89.8%)
V_{XC}(Li2–X6)	–15.4 (10.6%)	–14.7 (10.7%)	–13.1 (10.2%)
V^{IQA}(Li3–X6)	–128.3	–121.3	–111.0
V_C(Li3–X6)	–118.9 (92.7%)	–113.1 (93.2%)	–103.8 (93.5%)
V_{XC}(Li3–X6)	–9.4 (7.3%)	–8.2 (6.8%)	–7.2 (6.5%)
V^{IQA}(Li3–X7)	–136.7	–127.5	–118.1
V_C(Li3–X7)	–124.0 (90.7%)	–116.6 (91.5%)	–108.1 (91.5%)
V_{XC}(Li3–X7)	–12.7 (9.3%)	–10.9 (8.5%)	–10.0 (8.5%)

Table S3. AIM parameters (atomic units) for the bond critical points (BCPs) corresponding to the bonds in C_{2v} $SLi_4Cl_3^-$ (**1**) cluster.

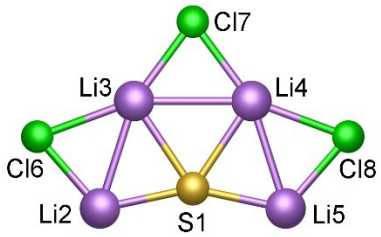

Bonds	$\rho(r)$	$\nabla^2\rho(r)$	H(r)	–G(r)/V(r)
S1–Li2	0.035	0.177	0.002	1.063
S1–Li3	0.022	0.103	0.003	1.133
Li2–Cl6	0.031	0.182	0.005	1.132
Li3–Cl6	0.020	0.110	0.004	1.209
Li3–Cl7	0.026	0.147	0.005	1.168

Table S4. AIM parameters (atomic units) for the bond critical points (BCPs) corresponding to the bonds in C_{2v} $SLi_4Br_3^-$ (**2**) cluster.

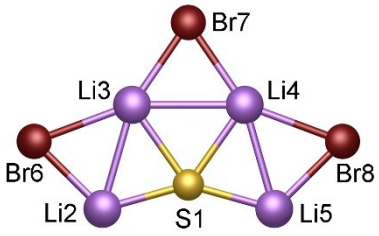

Bonds	$\rho(r)$	$\nabla^2\rho(r)$	H(r)	–G(r)/V(r)
S1–Li2	0.035	0.176	0.002	1.064
S1–Li3	0.023	0.110	0.003	1.128
Li2–Br6	0.027	0.133	0.003	1.105
Li3–Br6	0.017	0.079	0.002	1.170
Li3–Br7	0.022	0.107	0.003	1.136

Table S5. AIM parameters (atomic units) for the bond critical points (BCPs) corresponding to the bonds in C_{2v} $SLi_4I_3^-$ (**3**) cluster.

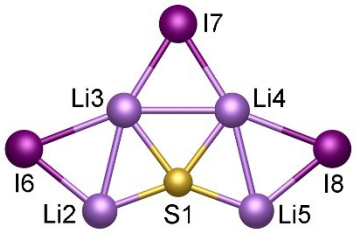

Bonds	$\rho(r)$	$\nabla^2\rho(r)$	H(r)	–G(r)/V(r)
S1–Li2	0.035	0.175	0.002	1.064
S1–Li3	0.024	0.117	0.003	1.122
Li2–I6	0.022	0.092	0.002	1.079
Li3–I6	0.013	0.053	0.001	1.140
Li3–I7	0.018	0.073	0.002	1.111

Figure S1. The AdNDP bonding pattern of $SLi_4Br_3^-$ (**2**) with occupation numbers (ONs, in |e|). (a) Nine lone pairs (LPs) of three Br atoms; (b) Three LPs of the S center; (c) Three 3c-2e Li–Br–Li σ bonds; (d) One 5c-2e σ bond.

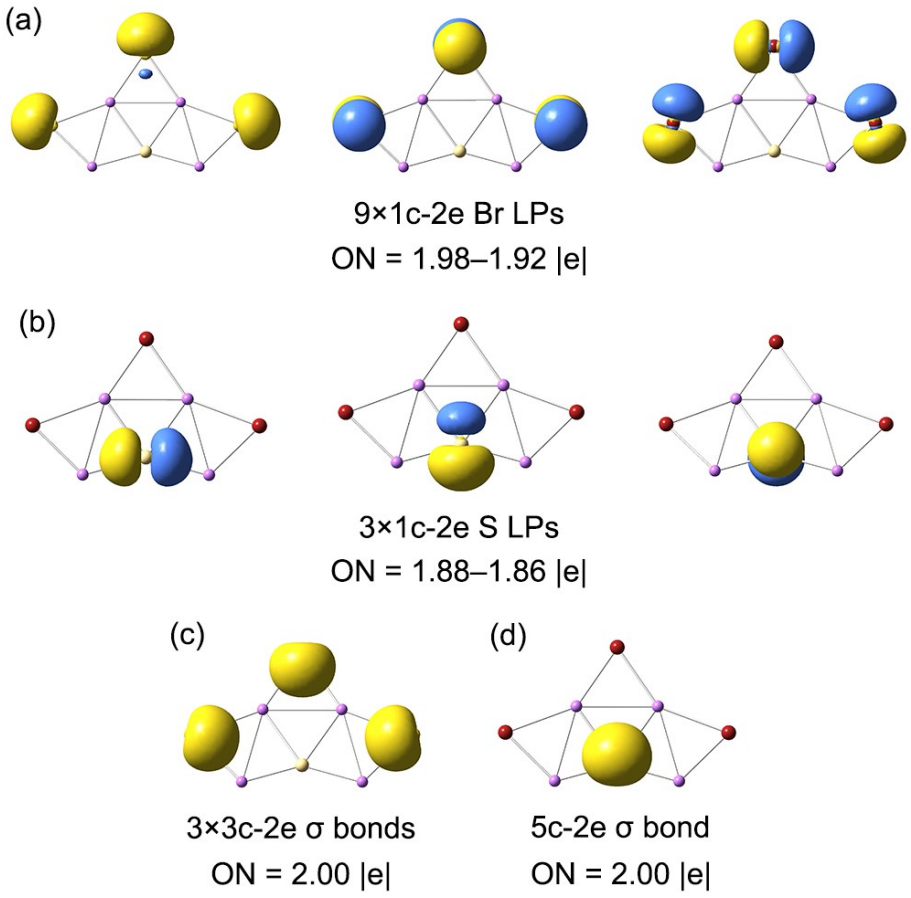

Figure S2. The AdNDP bonding pattern of $SLi_4I_3^-$ (**3**) with occupation numbers (ONs, in |e|). (a) Nine lone pairs (LPs) of three I atoms; (b) Three LPs of the S center; (c) Three 3c-2e Li–I–Li σ bonds; (d) One 5c-2e σ bond.

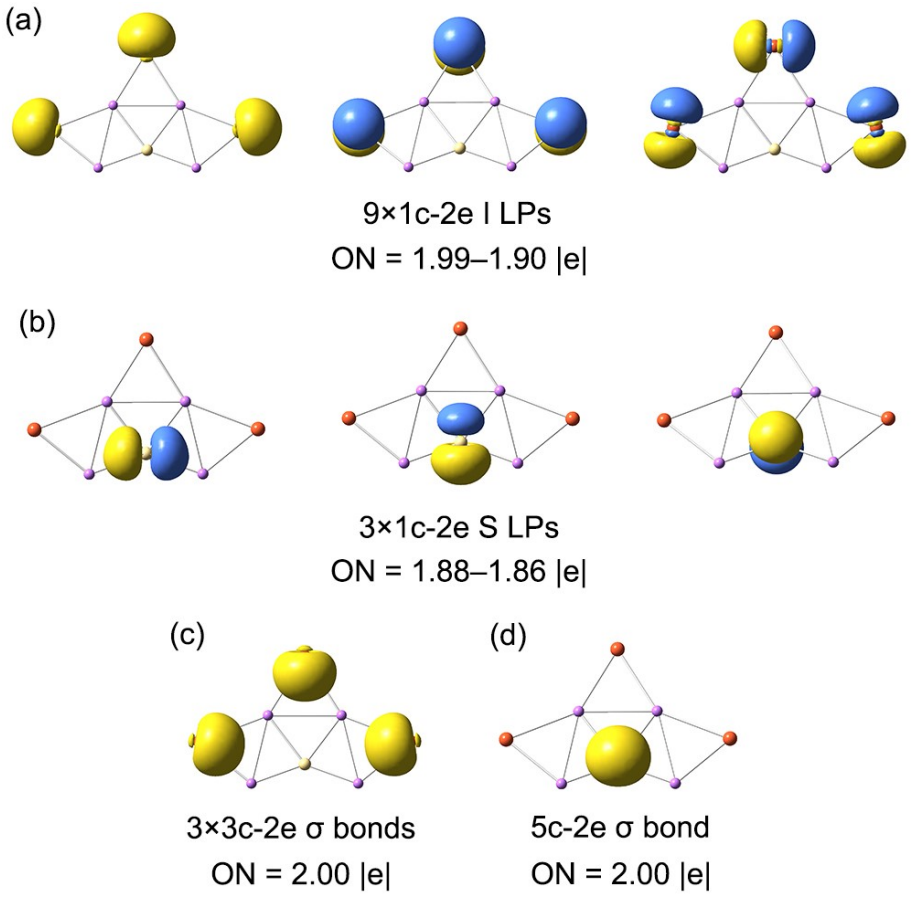

Figure S3. 2D plots of ELF and the contour line maps of Laplacian of electron density, bond paths and critical points of ptS **2** and **3**. The blue and red solid lines represent the positive and negative regions, respectively. The brown sticks between the atoms represent bond paths. The brown and yellow dots are bond and ring critical points, respectively.

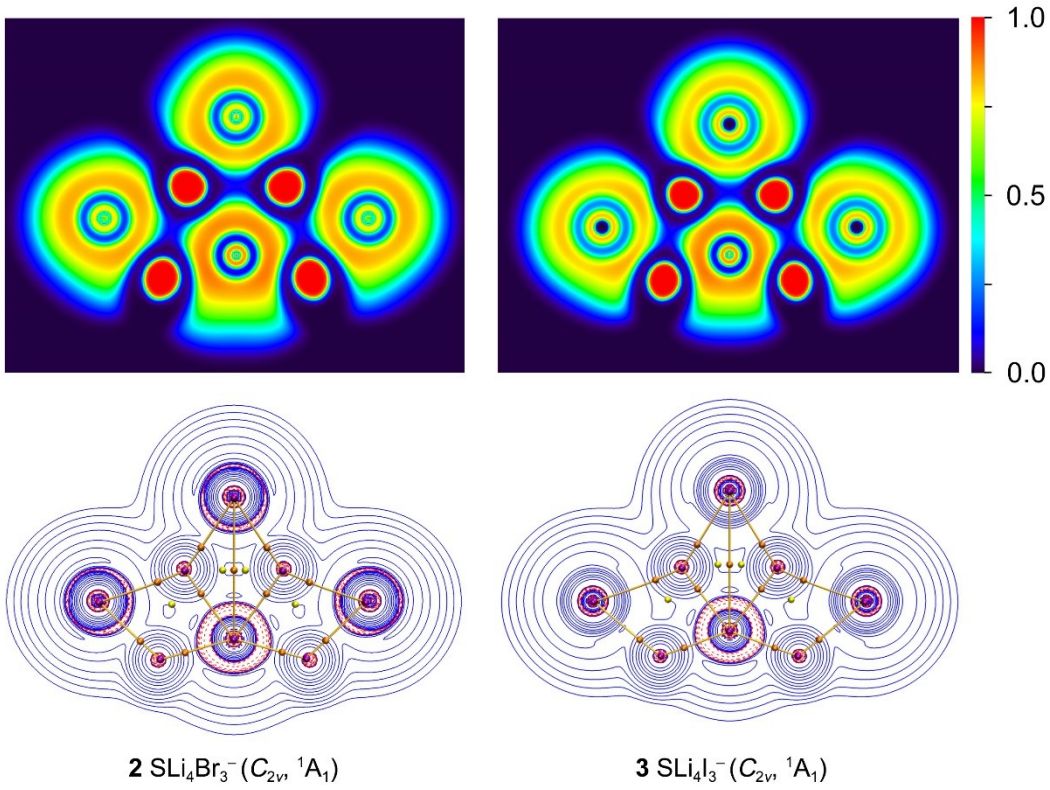

2 $SLi_4Br_3^-$ (C_{2v}, $^1A_1$) **3** $SLi_4I_3^-$ (C_{2v}, $^1A_1$)

Figure S4. Color-filled maps of $NICS(0)_{ZZ}$ and $NICS(1)_{ZZ}$ of the ptS **2, 3** clusters. 0 and 1 (in Å) represent the height above the molecular plane. Negative values indicate aromaticity.

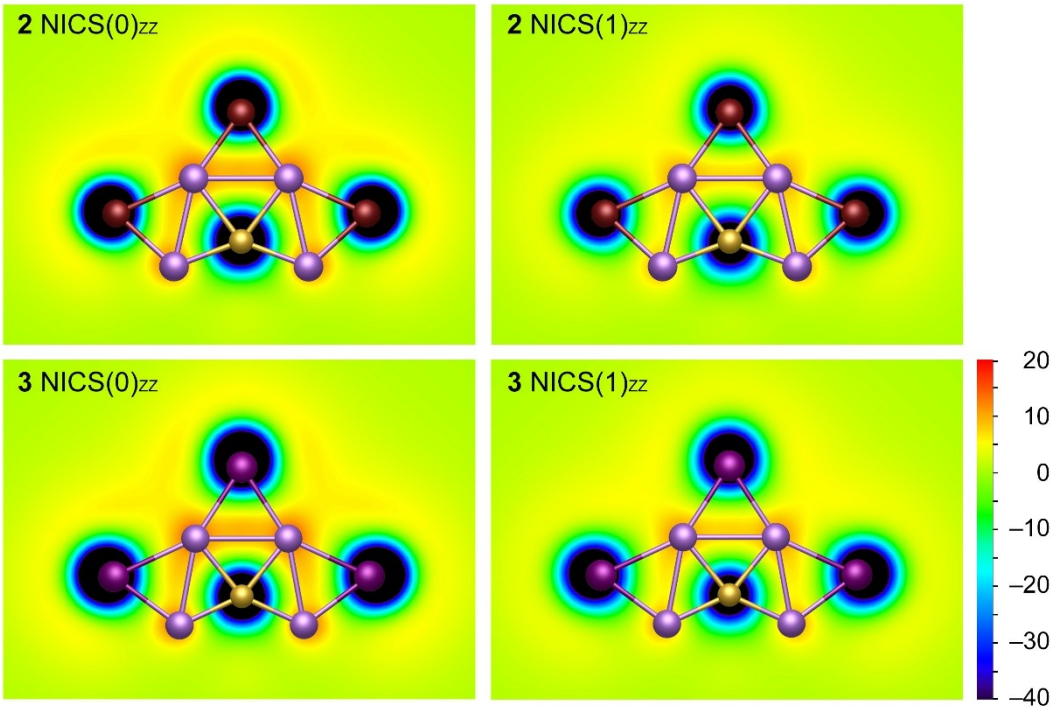

Cartesian coordinates of the top five low-lying isomers of $SLi_4X_3^-$ (X = Cl, Br, I) at the PBE0-D3(BJ)/def2-TZVPP level.

1 $SLi_4Cl_3^-$ (C_{2v}, $^1A_1$)

S	0.00000000	-1.44266400	0.00000000
Li	1.34681900	0.54954200	0.00000000
Li	2.12788400	-1.89155500	0.00000000
Li	-2.12788400	-1.89155500	0.00000000
Li	-1.34681900	0.54954200	0.00000000
Cl	-3.56355100	-0.26086800	0.00000000
Cl	3.56355100	-0.26086800	0.00000000
Cl	0.00000000	2.35318900	0.00000000

1B (C_{3v}, $^1A_1$)

S	0.00000000	0.00000000	2.54462500
Li	0.00000000	1.74531200	1.18080700
Li	0.00000000	0.00000000	-1.25689800
Li	1.51148500	-0.87265600	1.18080700
Li	-1.51148500	-0.87265600	1.18080700
Cl	0.00000000	2.29131400	-0.93275600
Cl	1.98433600	-1.14565700	-0.93275600
Cl	-1.98433600	-1.14565700	-0.93275600

1C (C_{3v}, $^1A_1$)

S	0.00000000	0.00000000	2.38524500
Li	0.00000000	0.00000000	-1.59571700
Li	0.00000000	1.53861000	0.76300900
Li	-1.33247600	-0.76930500	0.76300900
Li	1.33247600	-0.76930500	0.76300900
Cl	1.82624600	1.05438400	-0.78909500
Cl	0.00000000	-2.10876700	-0.78909500
Cl	-1.82624600	1.05438400	-0.78909500

1D (C_s, $^1A'$)

S	0.58023300	0.64545200	0.00000000
Li	0.66204800	-0.22263200	2.01966400
Li	0.53399300	-1.80103000	0.00000000
Li	-0.80567600	2.42944000	0.00000000
Li	0.66204800	-0.22263200	-2.01966400
Cl	-2.05591800	4.14587900	0.00000000

Cl	0.66204800	−2.39284200	2.22429900
Cl	0.66204800	−2.39284200	−2.22429900

1E (C_s, ^{1}A′)

S	−1.53588700	−0.25706500	0.00000000
Li	0.18709800	−1.35475700	1.13123900
Li	0.18709800	1.34391600	0.00000000
Li	−2.26890200	1.79541600	0.00000000
Li	0.18709800	−1.35475700	−1.13123900
Cl	−0.84100800	3.45607300	0.00000000
Cl	0.59927400	−3.28875400	0.00000000
Cl	1.98861800	−0.00122600	0.00000000

2 (C_{2v}, ^{1}A$_1$)

S	0.00000000	−1.65112600	0.00000000
Li	2.09680500	−2.23242000	0.00000000
Li	1.37408300	0.28846900	0.00000000
Li	−2.09680500	−2.23242000	0.00000000
Li	−1.37408300	0.28846900	0.00000000
Br	−3.76130600	−0.59703800	0.00000000
Br	0.00000000	2.28212400	0.00000000
Br	3.76130600	−0.59703800	0.00000000

2B (C_{3v}, ^{1}A$_1$)

S	0.00000000	0.00000000	2.98551600
Li	1.53517400	−0.88633300	1.67140000
Li	0.00000000	0.00000000	−0.85995100
Li	−1.53517400	−0.88633300	1.67140000
Li	0.00000000	1.77266600	1.67140000
Br	0.00000000	2.46480100	−0.57362900
Br	2.13458000	−1.23240000	−0.57362900
Br	−2.13458000	−1.23240000	−0.57362900

2C (C_s, ^{1}A′)

S	−0.41072200	−0.00016100	0.92103300
Li	0.38762100	−2.04475900	0.78538700
Li	1.77212500	0.00004100	−0.10935100
Li	−2.57395500	−0.00018500	0.29582100
Li	0.38725900	2.04458700	0.78542000
Br	2.49813600	−2.37554300	−0.17422300
Br	2.49772300	2.37574200	−0.17418500

Br	−4.80579000	−0.00009900	−0.22326000

2D (C_{3v}, $^1A_1$)

S	0.00000000	0.00000000	2.75084100
Li	1.36606500	0.78869800	1.18018400
Li	−1.36606500	0.78869800	1.18018400
Li	0.00000000	0.00000000	−1.28375300
Li	0.00000000	−1.57739600	1.18018400
Br	0.00000000	2.28813800	−0.48365600
Br	1.98158500	−1.14406900	−0.48365600
Br	−1.98158500	−1.14406900	−0.48365600

2E (C_s, $^1A'$)

S	−1.74019200	−0.28313400	0.00000000
Li	−0.07663200	−1.39630500	1.16686700
Li	−0.07663200	1.35687700	0.00000000
Li	−2.61710800	1.70833400	0.00000000
Li	−0.07663200	−1.39630500	−1.16686700
Br	−1.23473600	3.61212000	0.00000000
Br	0.34943100	−3.51459800	0.00000000
Br	1.92485000	0.00854500	0.00000000

3 (C_{2v}, $^1A_1$)

S	0.00000000	−1.69937900	0.00000000
Li	2.04564500	−2.44396100	0.00000000
Li	1.40971200	0.17685500	0.00000000
Li	−2.04564500	−2.44396100	0.00000000
Li	−1.40971200	0.17685500	0.00000000
I	−4.02346800	−0.82790600	0.00000000
I	0.00000000	2.42548600	0.00000000
I	4.02346800	−0.82790600	0.00000000

3B (C_s, $^1A'$)

S	0.70831200	0.85279000	0.00000000
Li	1.10230400	0.17607300	2.05434500
Li	0.67333600	−1.52517100	0.00000000
Li	−0.89279600	2.42625300	0.00000000
Li	1.10230400	0.17607300	−2.05434500
I	−2.53080500	4.34348900	0.00000000
I	1.10230400	−2.33593600	2.57134500
I	1.10230400	−2.33593600	−2.57134500

3C (C_{3v}, $^1A_1$)

S	0.00000000	0.00000000	3.23653500
Li	1.56877200	-0.90573100	1.99082100
Li	0.00000000	0.00000000	-0.64760100
Li	-1.56877200	-0.90573100	1.99082100
Li	0.00000000	1.81146200	1.99082100
I	0.00000000	2.69986700	-0.42615800
I	2.33815400	-1.34993400	-0.42615800
I	-2.33815400	-1.34993400	-0.42615800

3D (C_s, $^1A'$)

S	2.08745900	1.20396600	0.00000000
Li	1.65559300	-1.08565000	0.00000000
Li	0.33647100	0.80835600	1.45366700
Li	0.33647100	0.80835600	-1.45366700
Li	1.05683500	3.10328400	0.00000000
I	0.33647100	-1.64602900	-2.33910000
I	-1.49474300	2.72287900	0.00000000
I	0.33647100	-1.64602900	2.33910000

3E (C_s, $^1A'$)

S	-1.82133500	0.03181300	0.00000000
Li	-0.45806500	-1.36600600	1.21150200
Li	0.04595700	1.40455000	0.00000000
Li	-2.51255700	2.09220900	0.00000000
Li	-0.45806500	-1.36600600	-1.21150200
I	-0.83823200	4.04857200	0.00000000
I	-0.45806500	-3.77397800	0.00000000
I	2.03760900	-0.32748500	0.00000000